DOI: 10.1534/genetics.104.031914

Oligosyndactylism Mice Have an Inversion of Chromosome 8

Thomas L. Wise and Dimitrina D. Pravtcheva[1]

Department of Human Genetics, New York State Institute for Basic Research in Developmental Disabilities, Staten Island, New York 10314

Manuscript received June 1, 2004
Accepted for publication August 4, 2004

ABSTRACT

The radiation-induced mutation *Oligosyndactylism* (*Os*) is associated with limb and kidney defects in heterozygotes and with mitotic arrest and embryonic lethality in homozygotes. We reported that the cell cycle block in *Os* and in the 94-A/K transgene-induced mutations is due to disruption of the *Anapc10* (*Apc10/Doc1*) gene. To understand the genetic basis of the limb and kidney abnormalities in *Os* mice we characterized the structural changes of chromosome 8 associated with this mutation. We demonstrate that the *Os* chromosome 8 has suffered two breaks that are 5 cM (~10 Mb) apart and the internal fragment delineated by the breaks is in an inverted orientation on the mutant chromosome. While sequences in proximity to the distal break are present in an abnormal *Os*-specific *Anapc10* hybrid transcript, transcription of these sequences in normal mice is low and difficult to detect. Transfer of the *Os* mutation onto an FVB/N background indicated that the absence of dominant effects in 94-A/K mice is not due to strain background effects on the mutation. Further analysis of this mutation will determine if a gene interrupted by the break or a long-range effect of the rearrangement on neighboring genes is responsible for the dominant effects of *Os*.

CONGENITAL limb malformations are the second most common birth defect in humans (after heart malformations), with a frequency of 1/1000 newborns (Manouvrier-Hanu *et al.* 1999). Several hundred human syndromes involving various types of limb deformity have been described; syndactyly is the most common deformity involving the hand (Barsky 1958). So far at least 20 different genes have been shown to play a role in these syndromes (Gurrieri *et al.* 2002), but in many cases the identity of the affected genes remains unknown.

Numerous mutations that affect digit development have been identified in mice (Lyon *et al.* 1996). One of these mutations, discovered in the progeny of an irradiated male, is *Oligosyndactylism* (*Os*; Grüneberg 1956). Two types of dominant developmental effects are associated with this mutation: (i) fusion of the second and third digits on all four limbs, accompanied by fusions of metacarpal/metatarsal and carpal/tarsal bones and abnormal attachments of muscles in the distal limbs (Grüneberg 1956, 1961; Kadam 1962), and (ii) a reduced number of nephrons in the kidney (Falconer *et al.* 1964; Stewart and Stewart 1969; Zalups 1993), leading to nephrogenic urine concentration defects, which in some strains manifest as diabetes insipidus (Stewart and Stewart 1969). The mouse *Os* mutation thus may be useful for identifying one or more genes that affect renal mass. This is clinically important because bilateral renal hypoplasia is the fourth most common cause of renal failure in childhood (Bernstein 1992; Sorenson *et al.* 1996). In addition to the dominant effects on limb and kidney development, the *Os* mutation has a recessive effect on viability: homozygous *Os/Os* embryos die around the time of implantation, as a result of cell cycle block at the metaphase/anaphase transition (Van Valen 1966; Paterson 1979; Magnuson and Epstein 1984; Yee *et al.* 1987; Hiraoka *et al.* 1989).

The *Os* mutation has been genetically mapped to mouse chromosome 8 (Ceci and Mills 1997). We identified two related transgene-induced mutations (94-A and 94-K) that map to the same region of chromosome 8. Genetic and phenotypic analysis indicated that the 94-A/K mutations represent new alleles of the gene causing mitotic arrest in *Os/Os* cells (Pravtcheva and Wise 1995, 1996). cDNA selection with BAC clones from this region and analysis of the selected cDNAs indicated that the 94-A/K and *Os* mutations disrupt the gene encoding component 10 of the anaphase-promoting complex/cyclosome (APC/C; Hwang and Murray 1997; Kominami *et al.* 1998; Grossberger *et al.* 1999; Pravtcheva and Wise 2001). This gene, *Anapc10*, was previously referred to as *Apc10* or *Doc1* (*d*estruction *o*f *c*yclin B mutant *1*). APC/C is a ubiquitin ligase (Irniger *et al.* 1995; King *et al.* 1995; Sudakin *et al.* 1995), and its function is essential for the proteolytic destruction of several proteins that must take place for the cell cycle to proceed beyond metaphase (King *et al.* 1996; Morgan 1999; Nasmyth *et al.* 2000). Nonmitotic functions of APC/C have also been described

[1]*Corresponding author:* Department of Human Genetics, NYS Institute for Basic Research in Developmental Disabilities, Staten Island, NY 10314. E-mail: bgyanyib@earthlink.net

(Konishi *et al.* 2004; Wirth *et al.* 2004). APC10 is believed to contribute to substrate recognition (Passmore *et al.* 2003). The activity of APC/C is regulated by the spindle assembly checkpoint, which monitors spindle structure and chromosome alignment and prevents the emergence of aneuploidy. The disruption of this gene can explain the mitotic arrest phenotype of the 94-A/K and *Os/Os* cells. Chromosome mapping with human/rodent hybrids containing single human chromosomes and examination of the published human genome sequence indicated that the human ortholog of this gene (*ANAPC10*) resides on human chromosome 4 (Pravtcheva and Wise 2001).

Southern analysis of DNA from 94 A/K transgenic mice with probes from the *Anapc10* region indicated that both of the transgene insertions had caused deletions within the gene and result in its functional inactivation. Correspondingly, 94-A and 94-K heterozygotes showed decreased dosage of the *Anapc10* mRNA (Pravtcheva and Wise 2001). The normal phenotype of 94-A and 94-K heterozygous mice indicated that haplo-insufficiency of *Anapc10* on an FVB/N background is not associated with limb and kidney defects as seen in *Os* mice.

Southern analysis of genomic DNA from *Os* mice indicated that the *Anapc10* gene is rearranged in *Os* mice with no evidence for a deletion. Heterozygous *Os* mice also showed a decrease in the level of the normal *Anapc10* mRNA and, in addition, the presence of an abnormal, shorter *Anapc10* mRNA species (Pravtcheva and Wise 2001). We have sequenced a 3′ rapid amplification of cDNA ends (RACE) clone corresponding to this novel mRNA species and have determined that sequences following *Anapc10* exon 4 are missing from this mRNA and are replaced by a short 150-nt fragment unrelated to *Anapc10*. The sequences absent from the shorter *Anapc10* mRNA encode a highly conserved portion of the APC10 protein, which led us to conclude that the protein encoded by the short mRNA species would be inactive. This inactivity would account for the mitotic arrest in homozygous *Os/Os* embryos.

These results indicated the involvement of a second genomic region in the *Os* mutation. Defining the exact nature of the rearrangement will help us understand the genetic basis of the more complex phenotype of *Os* mice. We therefore isolated genomic clones containing the *Os*-specific transcript novel sequence, determined the position of these clones on the genetic and physical map of chromosome 8, and carried out a structural analysis aimed at defining the type of rearrangement that has resulted in the production of a hybrid transcript. We have also transferred the *Os* mutation onto an FVB/N background. The resulting phenotype indicated that the dominant effects of *Os* are not due to strain-specific effects of *Anapc10* haplo-insufficiency. Our analysis provides further evidence that the *Os* mutation is associated with a chromosome inversion and suggests several genes that need to be examined as candidates for the dominant *Os* phenotype.

MATERIALS AND METHODS

Mice: FVB/N mice were purchased from Taconic Farms (Germantown, NY). Mice with the *Os* mutation were obtained from the Jackson Laboratory. The original strain used in our analysis of the relationship between the 94-A/K transgene mutations and *Os* was ROP/GnLeJ (Pravtcheva and Wise 1996). In more recent experiments, we have used the ROP/Le-*Os Es 1^a/+ Es 1^a*/J strain or progeny from backcrossing this strain with FVB/N mice. Cby.RBF-Rb(8.12)5Bnr mice [referred to as Rb(8.12)] were obtained from the Jackson Laboratory. Strain 101 DNA was obtained from the Oak Ridge National Laboratory.

DNA isolation: Plasmid and BAC DNAs were isolated by the alkaline lysis procedure (Sambrook *et al.* 1989). Genomic DNA from cells, tissues, and embryos was isolated by standard methods (Sambrook *et al.* 1989; Hogan *et al.* 1994).

Southern hybridization: DNA was digested to completion with restriction endonucleases, electrophoresed on agarose gels, denatured, and transferred to nitrocellulose or nylon filters. The filters were prehybridized, hybridized, and washed as described by Sambrook *et al.* (1989). Probes were radiolabeled by the random primer method (Feinberg and Vogelstein 1983). *Anapc10* cDNAs and genomic region probes were previously described (Pravtcheva and Wise 2001). The following additional probes were used: *Xho*I/*Bgl*II fragment of EST AI930292 for analysis of the *Abce1* gene, *Not*I/*Sal*I excised insert of EST BU053222 for analysis of the *Hhip* gene, and *Not*I/*Sal*I excised insert of EST AI426947 for analysis of *Sall1*.

Northern hybridization: Total RNA was isolated from cells, tissues, and embryos using Trizol reagent (Invitrogen, Carlsbad, CA; Chomczynski and Sacchi 1987). RNA was then electrophoresed in agarose gels containing 0.66 m formaldehyde and transferred to nylon filters as described by Davis *et al.* (1986).

Amplification of genomic DNA: Standard PCR was done by the method of Saiki (1990) as described in Wise and Pravtcheva (1997). Primers for mapping the 500-9 region were CAGCCTAGGTTTATTTATCA and CCCAGGATGCAA CAGTAATG. Long PCR was done by the method of Cheng *et al.* (1995). Primers used to show the inversion at the proximal breakpoint were TTGTCTCTGTGCCCTCTAGT and TACA TAAACCAACGGAACAAC. Primers used to show the inversion at the distal breakpoint were AGGGCTCCATACTCAAATAGG and GAAAGGCAGCCCAATGTCTAC.

Amplification of RNA: RT-PCR was done as described previously (Wise and Pravtcheva 1997). Primers for RT-PCR of the 500-9 sequence were CAGACCCACCTCCACCTACT and CAGCCTAGGTTTATTTATCA.

Rapid amplification of cDNA ends: The 5′ ends of mRNAs were amplified using a modification of the original RACE protocol (Frohman 1990; Invitrogen kit) or by RNA ligase-mediated RACE [Maruyama and Sugano 1994; Ambion (Austin, TX) or Invitrogen kits] with a gene-specific primer and a primer complementary to the adapter primer.

cDNA selection: The cDNAs encoded by BACs were identified by cDNA selection (Peterson 1998; Pravtcheva and Wise 2001).

DNA sequencing: DNA was sequenced by the dye terminator cycle sequencing method (Beckman Coulter, Fullerton, CA).

Screening of cDNA and genomic libraries: DNA and genomic phage libraries were screened as described in Sambrook *et al.* (1989). BAC clones homologous to the 500-9 novel sequence were identified by screening a Genome Systems BAC library from 129/Sv ES cells.

Preparation of 96h13 BAC DNA for injection: 96h13 BAC DNA was prepared in agarose plugs, digested with λ-terminase and run on a pulsed field gel. The linearized fragment was

then electroeluted from the gel slice, dialyzed in 10 mm Tris, pH 7.5, 0.1 mm EDTA, and diluted to a concentration of 0.6 μg/ml for injection.

Micro-injection of DNA into early embryos: FVB/N embryos were micro-injected as described by Hogan *et al.* (1994). Transgenic founders were identified by PCR with vector primers CTTTAGGGAAATAGGCCAGGTTT and AAAAATCACT GGATATACCACCG. The transgenes were maintained on an FVB/N background.

Karyotype analysis: Two types of *Os* cells were used for chromosome analysis: (i) a liver cell culture established from a newborn *Os* mouse and (ii) an embryo cell culture from a cross between Rb(8.12) homozygous male and an *Os*/+ female mouse. Embryos were removed on day 15 (day 1 is day of morning plug). Individual embryos were examined under a microscope and classified as *Os*/+ or +/+ on the basis of the limb morphology. The embryos were torn into small pieces and placed into individual T25 flasks marked as *Os*/+ or +/+ on the basis of the limb phenotype. The tissue culture medium was αMEM plus 15% fetal calf serum. One week later the cells were transferred into a T75 flask and upon reaching confluence were frozen. A culture established from a frozen ampule was used for karyotyping after one passage. Chromosome spreads were prepared and G-banded using standard techniques.

RESULTS

Involvement of a second chromosome region in the *Os* mutation: Several tissues of *Os* mice expressed an abnormal, shorter (500 bp) *Anapc10* mRNA species and decreased levels of the normal (800 bp) *Anapc10* mRNA (Pravtcheva and Wise 2001). As indicated in the introduction, sequencing of a 3′ RACE clone corresponding to this novel mRNA indicated that the 3′ end of the *Anapc10* mRNA is replaced by a 150-nt fragment unrelated to the *Anapc10* gene (for brevity we will refer to this novel sequence as 500-9, from the designation of the sequenced RACE clone). The 500-9 sequence was not present in any of the BACs containing the *Anapc10* gene (by PCR and Southern hybridization analysis), indicating that 500-9 had originated from a genomic region outside of these BACs. To isolate a genomic clone that contains the 500-9 novel sequence we screened a mouse BAC library (Genome Systems) with the 500-9 probe and isolated four BAC clones that showed homology to the probe. A fifth BAC clone (68i8) was identified in the public database. A 16-kb *Hin*dIII BAC subfragment that contains the 500-9 sequence was subcloned and sequenced. Primers bracketing a polymorphic *Sac*I site in this sequence were used to screen the Jackson Laboratory BSS panel, to determine the exact position of this region on the mouse genetic map. This analysis indicated that the 500-9 sequence is at 42 cM, which is ~5 cM distal to *Anapc10* (at 37 cM). The distance between *Anapc10* and 500-9 on the chromosome 8 sequence in Map Viewer (http://ncbi.nlm.nih.gov) is ~10 Mb (see below). This indicates that the *Os* chromosome has rearranged to bring *Anapc10* and 500-9 closer together.

Several types of rearrangement may bring normally distant sequences closer: (i) a deletion with one breakpoint in the *Anapc10* region and another one ~5 cM away (loss of a chromosome segment of this size would be expected to visibly alter the morphology of the mutant chromosome), (ii) insertional translocation of a chromosome segment from a region that is 5 cM distal to the *Anapc10* gene into the *Anapc10* locus, and (iii) a chromosome inversion with one break in the *Anapc10* region and another one 5 cM away. The latter two rearrangements may or may not affect the chromosome morphology, depending on the exact position of the breaks and the size of the inserted or inverted fragment. It is also possible that the *Os* mutation is associated with more than one type of rearrangement (*e.g.*, deletion of sequences in addition to an inversion or insertion of an inverted chromosome fragment). We attempted to determine which of the proposed rearrangements has taken place in *Os* mice by molecular genetic analysis of the mutation.

***Os* mice have no major loss of sequences from the 94-A/K (*Anapc10*) region:** As reported previously, probes from the region around one end of the 94-A and 94-K deletions (probes a and b in Figure 1A) detected novel fragments in *Os* mice after *Hin*dIII or *Sac*I digests, suggesting a rearrangement (Pravtcheva and Wise 1996, 2001). On the other hand, hybridization of Southern blots of *Os* DNA with other probes from the 94-A/K (*Anapc10*) region showed no evidence for rearrangements or loss of sequences. Hybridization of cDNA 112 with *Bam*HI-digested *Os*/+ and wt DNA is shown in Figure 1B. This cDNA clone contains sequences of *Anapc10* exons 2–5. The largest *Bam*HI fragment recognized by this cDNA (exon 5) is polymorphic (f and f′ in Figure 1B) and is >12 kb in FVB/N mice (fragment f) and ~11 kb on both the normal and the mutant chromosome 8 in the ROP/GnLe strain (fragment f′). The *Os*/+ mice shown in the first two lanes, produced from a cross between ROP/GnLe *Os*/+ and FVB/N mice, contain both the f and the f′ variants, as does one of the normal mice shown in lane 3. The other normal mouse shown in lane 4 is from a different cross and contains two copies of the larger FVB/N f fragment, with a correspondingly stronger signal. This polymorphism is further illustrated in Figure 1B, right, which contains *Bam*HI digests of DNA from *Os*/+ and +/+ mice from strain ROP/Le *Os Es1*^{a}/+ *Es1*^{a}/J (first three lanes), and FVB/N (fourth lane). None of the hybridizing fragments appears rearranged or weakened in the mutant mice. Three of the fragments hybridizing to this probe (indicated by asterisks in Figure 1B, left) are not present on blots of *Anapc10* region BACs and represent related sequences located on other chromosomes (see Figure 1 legend). These unlinked fragments can be used as a control for loading. These results indicate that the *Os* mutation is associated with a break in the continuity of the DNA in the region adjacent to probes a and b and rejoining of the broken ends with DNA with a different restriction site composi-

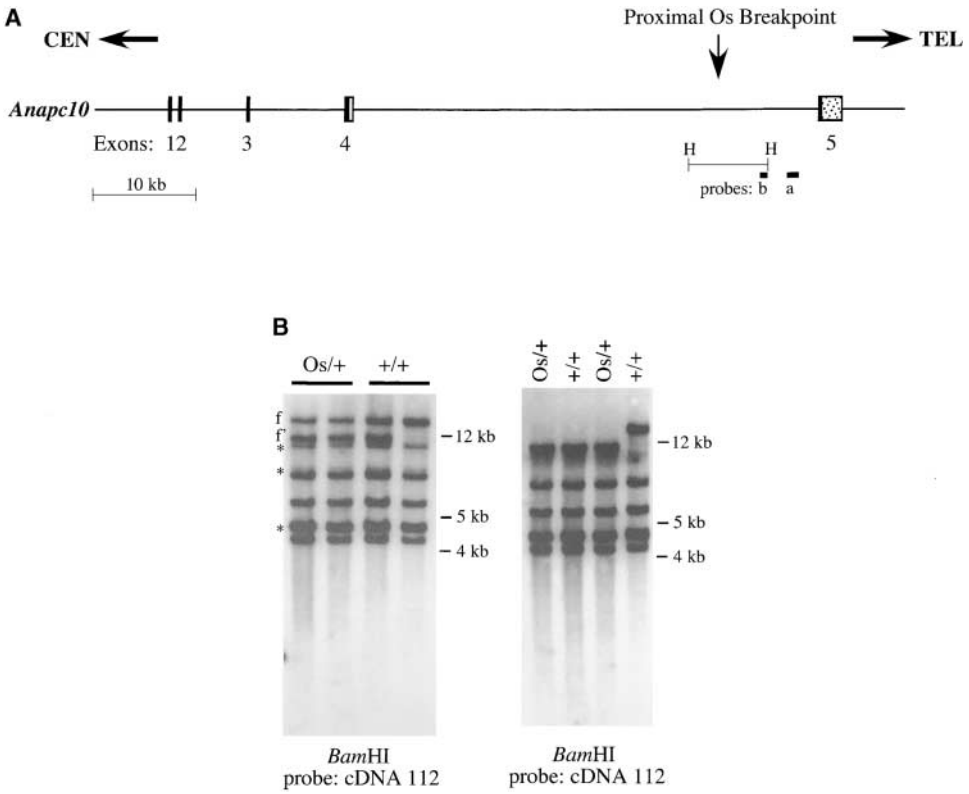

FIGURE 1.—Sequences surrounding the proximal *Os* breakpoint are retained in *Os* mice. (A) Structure of the *Anapc10* gene. Vertical rectangles mark the position of exons. These positions were determined by comparing the sequence of BAC 59K2 selected cDNAs with the sequence of the NT_039467 contig. They are in good agreement with the sequence of 1500026N15Rik (corresponding to *Anapc10*), although one of our selected cDNAs has a longer exon 4 (shown as gray portion), and the last exon of the selected cDNAs is shorter than the exon of the predicted gene (whose full length would include the stippled portion). These may represent alternatively spliced/polyadenylated transcripts from this locus. The smaller size of the last exon is supported by the size of the predominant transcript detected with *Anapc10* probes (PRAVTCHEVA and WISE 2001). The position of the *Hin*dIII fragment containing the proximal *Os* breakpoint (PRAVTCHEVA and WISE 2001) is indicated below the line. Solid bars mark the position of genomic probes a and b used in the analysis of the rearrangement (see text). (B) Southern analysis of mutant and control mice with *Anapc10* cDNA 112, which contains exons 2–5. The DNA was digested with *Bam*HI. Fragments f and f′ represent an allelic polymorphism. The first three lanes on the left contain DNA from ROP/GnLe mice crossed with FVB/N, whereas the first three lanes on the right are from ROP/Le *Os Es 1*^{a}/+ *Es 1*^{a} mice; the fourth lane on both sides contains DNA from FVB/N mice. The presence (Os/+) or absence (+/+) of the mutation is indicated above each lane. Asterisks mark unlinked fragments. The fragment showing the strongest hybridization (~4–5 kb) corresponds to an intronless copy of *Anapc10* on chromosome 16 (PRAVTCHEVA and WISE 2001); the larger of the remaining two weak fragments (migrating slightly ahead of f′ and visible more clearly in the last lane) corresponds to an uncharacterized region of sequence homology on chromosome 9 (D. D. PRAVTCHEVA and T. L. WISE, unpublished observations). The chromosomal location of the weakest fragment, which is not seen on all blots, is currently unknown.

tion. There is no evidence for loss or rearrangement of sequences 5′ (exons 2–4) or 3′ (exon 5) from this break (Figure 1B). This conclusion is in agreement with the finding of an abnormal transcript containing *Anapc10* exons 1–4 in *Os* mice. Therefore the more complex phenotype of *Os* mice cannot be explained by a large deletion in the *Anapc10* region that overlaps with the deletion in 94-A/K mice but extends further to encompass additional genes.

No significant loss of sequences in the distal *Os* breakpoint region: We have subcloned several smaller fragments from the 16-kb *Hin*dIII fragment that contains the 500-9 novel sequence and used these subclones as probes on Southern blots to determine if they detect rearrangements or deletions in *Os* mice. Several cDNAs (see below) mapping to the 16-kb *Hin*dIII fragment were also used as probes (Figure 2A). One of these cDNA clones (R1/R5, which contains the unspliced 500-9 sequence) hybridizes to the expected 16-kb *Hin*dIII fragment and, in addition, to a smaller fragment that segregates with the *Os* mutation (Figure 2B). Further analysis using the subclones or selected cDNAs that map within the 16-kb fragment indicated that *Eco*RI fragment 3 and probes to the left detect the same novel fragment as the 500-9 novel sequence cDNA (designated Os-A in Figure 2B), whereas probes to the right detect a different novel fragment designated Os-B [in addition to the 16-kb fragment present on the wild-type (wt) chromosome 8; Figure 2C]. Southern hybridization of *Eco*RI-digested *Os*/+ and +/+ DNA hybridized with *Eco*RI fragment 3 is shown in Figure 2E. The probe detects two novel fragments in *Os* mice (indicated by arrows) in addition to the fragment from the normal chromosome 8. This is the expected outcome of a break within the *Eco*RI fragment 3 and rejoining of the broken ends with sequences with different restriction site composition.

It has been reported that the *Os* chromosome 8 shows suppression of recombination over a large centrally located segment. This nonrecombining segment contains sequence polymorphisms characteristic of strain 101, from which the mutant chromosome 8 was derived (LENZ *et al.* 1998). Such polymorphisms will segregate

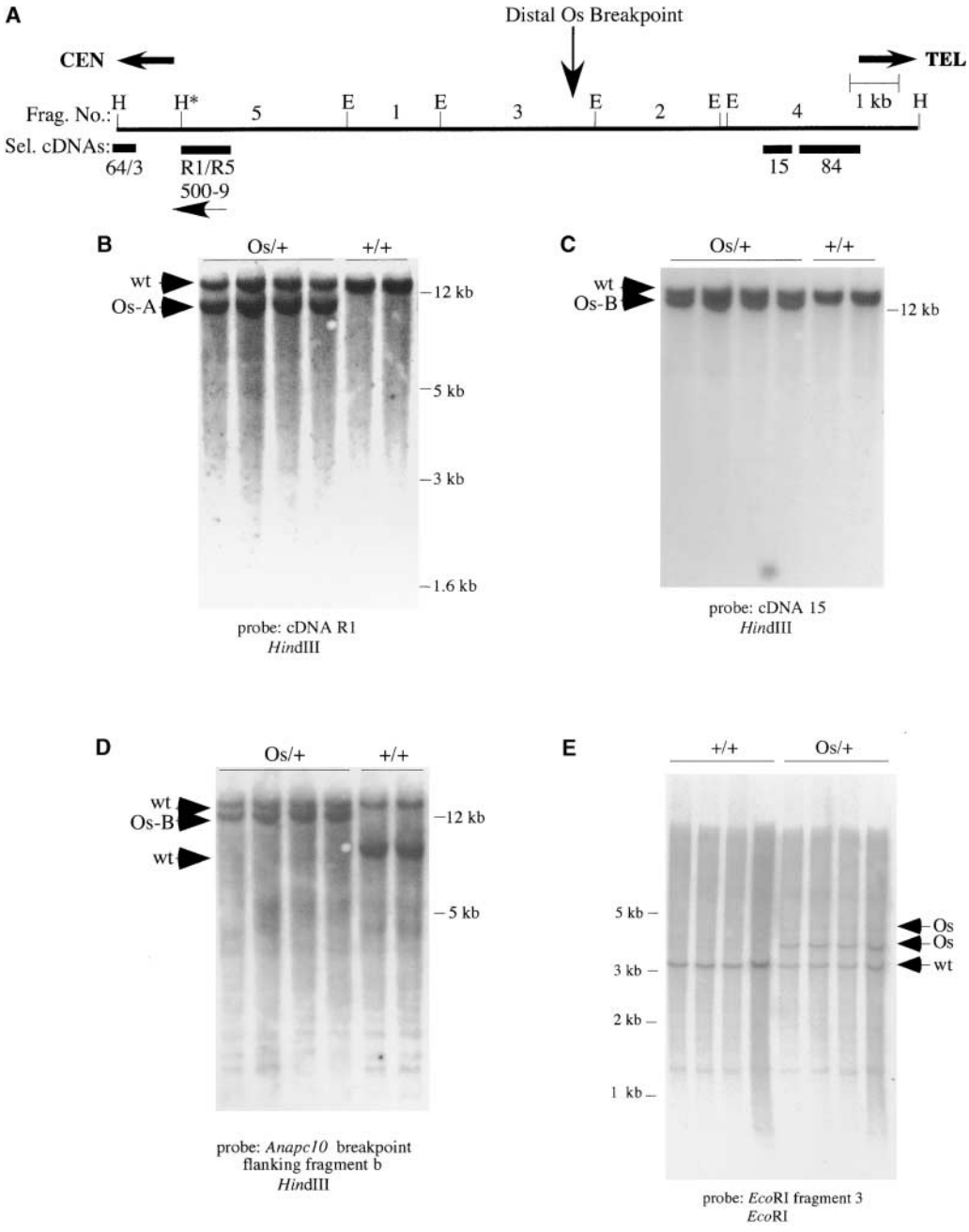

FIGURE 2.—Structural analysis of *Os* DNA with cDNA or genomic probes from the 500-9 homologous BACs. (A) *Eco*RI restriction map of the 16-kb *Hin*dIII fragment that contains the 500-9 novel sequence. The position of the restriction sites was confirmed by sequencing. The fragment was oriented by comparison with the sequence of contig NT_081826 and is shown in a (left to right) centromere-to-telomere orientation. The *Eco*RI fragments are numbered according to size (1–5). A polymorphic *Hin*dIII site present in C57BL/6 and some other strains is indicated with an asterisk. Solid rectangles below the line mark the position of cDNAs (isolated by cDNA selection or library screening), as determined by sequencing. The 500-9 novel sequence is contained within cDNA clone R1/R5. The arrow underneath 500-9 indicates the 5′ to 3′ orientation of the sequence in the 500-9 hybrid transcript. The position of the breakpoint in *Eco*RI fragment 3 is indicated above the line. (B–D) Rearrangements in *Os*/+ mice detected following *Hin*dIII digestion. (B) Rearrangement detected with cDNA clone R1/R5. (C) *Os*-specific novel fragment detected with cDNA 15. (D) *Os*-specific novel fragment detected with *Anapc10* region probe b (Figure 1A). Mouse DNA was digested with *Hin*dIII and Southern blots were hybridized with the indicated cDNA or genomic probes. All samples in B–D are from progeny of an ROP/GnLe × FVB/N cross. Os/+ lanes contain DNA from mutant mice; +/+ lanes contain DNA from normal mice. Wt indicates the normal fragment recognized by the probe. Os-A and Os-B designate the two novel fragments homologous to the probes in *Os* mice. All probes were consecutively applied to the same blot. As previously reported (PRAVTCHEVA and WISE 1996), *Anapc10* region probe b detects a *Hin*dIII fragment that is polymorphic between the normal ROP/GnLe chromosome 8 (where it has a size of ~8 kb) and FVB/N mice (>12 kb size). Mutant mice in this cross have the large FVB/N fragment and fragment Os-B, whereas normal mice have the FVB/N fragment and the smaller ~8-kb fragment from the ROP/GnLe strain normal chromosome 8. (E) Southern analysis of *Eco*RI-digested *Os*/+ and +/+ DNA with *Eco*RI fragment 3. Arrows indicate the position of the two novel fragments detected in *Os*/+ mice. The lower-molecular-weight band seen in all the lanes represents cross-hybridizing sequences located elsewhere in the genome.

with the mutation, even though they may be located at a significant distance from the actual breakpoints. We had previously examined a number of different mouse strains for polymorphisms in the 94-A/K region (PRAVTCHEVA and WISE 1996). Examination of the same set of strains with probes from the 16-kb *Hin*dIII fragment did reveal a polymorphism, most clearly illustrated after hybridization with cDNA clone 64/3. Several strains, including A/HeJ, C3H, C57BL/6, and the normal chromosome 8 of the ROP/GnLe strain, contain a short, 1.3-kb *Hin*dIII

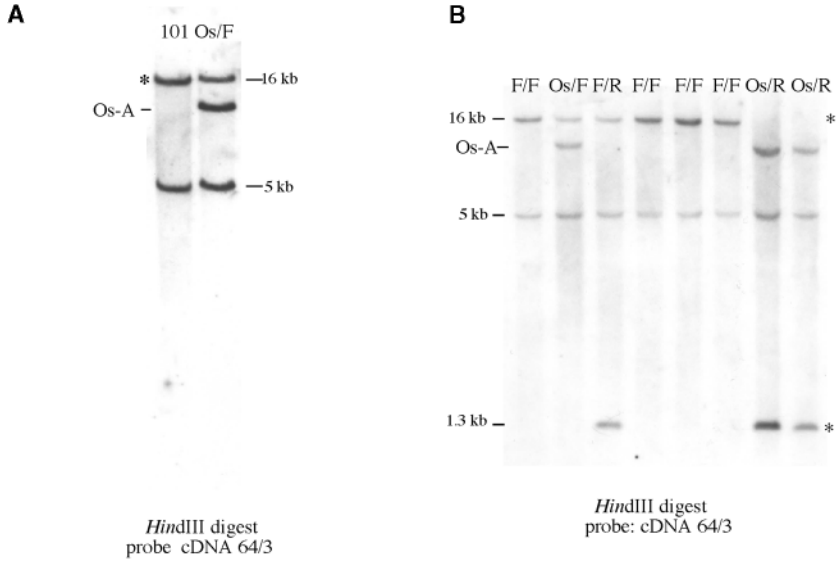

FIGURE 3.—Strain polymorphism of the 16-kb *Hin*dIII fragment. The polymorphic fragment is indicated by an asterisk. (A) DNA of a strain 101 mouse and an *Os* mouse backcrossed with FVB/N (lane Os/F), probed with cDNA clone 64/3. (B) DNA from mice containing the FVB/N chromosome 8 (F), normal ROP/GnLe chromosome 8 (R), or the mutant chromosome 8 (Os) probed with cDNA clone 64/3. This cDNA extends beyond the 16-kb *Hin*dIII fragment and detects an additional nonpolymorphic fragment of ~5 kb. The large *Hin*dIII fragment present in 101 mice has the same size as the normal FVB/N fragment and is distinct from the mutation-associated fragment Os-A; the normal chromosome 8 in the ROP/GnLe strain has the polymorphic *Hin*dIII site (Figure 2A) resulting in the ~1.3-kb fragment hybridizing to the probe.

fragment, whereas the large 16-kb *Hin*dIII fragment is present in AKR, BALB/c, CBA, SJL, 129, 101, and FVB/N mice (fragments present in FVB/N, 101, and ROP/GnLe are illustrated in Figure 3, A and B). This polymorphism is due to the presence/absence of a *Hin*dIII site close to the proximal end of the 16-kb *Hin*dIII fragment (Figure 2A). cDNA 64/3 extends beyond the end of the 16-kb *Hin*dIII fragment and also hybridizes to the adjacent nonpolymorphic fragment of ~5 kb. Strains that contain the short *Hin*dIII fragment detected with cDNA clone 64/3 (*e.g.*, the normal chromosome 8 in ROP/GnLe mice) show a slight decrease in the size of the normal fragment hybridizing with cDNA clones to the right of the polymorphic *Hin*dIII site (R1/R5, 15, and 84; not shown). These results demonstrate that the Os-A and Os-B fragments represent rearrangements specific to the mutant *Os* chromosome and not a polymorphism specific for the 101 strain of mice.

***Os* is associated with a chromosome inversion:** Several lines of evidence indicate that the rearrangement in *Os* is a chromosome inversion of the fragment between the breaks in the *Anapc10* and the 500-9 regions: (i) On the normal chromosome 8 the 500-9 novel sequence is located ~10 Mb away from the *Anapc10* locus, on the centromeric side of the distal break (http://ncbi.nlm.nih.gov; Figures 2A and 6, A and C). The orientation of the normal 500-9 sequence is opposite to the orientation of the *Anapc10* transcript. The production of a hybrid transcript indicates that on the *Os* chromosome 8 the distal end of the 10-Mb fragment is joined to *Anapc10* exons 1–4 in an inverted orientation. (ii) Probes on the telomeric side of the *Anapc10* break (probe b in Figure 1A) and on the telomeric side of the 500-9 region break (cDNA 15) detect the same novel fragment in *Os* mice (Figure 2, A, C, and D). (iii) We have been able to amplify *Os*-specific fragments by PCR with primer pairs that span the proximal and distal chromosome 8 breaks. The primers for each PCR are normally 10 Mb apart and run in the same direction on normal chromosome 8 (Figure 4A). We first amplified a 10-kb PCR product from the distal breakpoint (Figure 4C). Our Southern analysis indicated that this PCR product should contain a 4.3-kb *Eco*RI fragment (Figure 2E) that contains the breakpoint, so we subcloned this fragment and sequenced it (Figure 5A). The sequence indicates that the centromeric side of the distal breakpoint contains an inverted sequence precisely from the region of the normal chromosome that is 10 Mb away on the telomeric side of the proximal breakpoint. We then used this sequence information to design primers that amplify a fragment spanning the proximal breakpoint (Figure 4B) and sequenced the fragment (Figure 5B). The sequence indicates that the telomeric side of the proximal breakpoint contains an inverted sequence precisely from the region of the normal chromosome that is 10 Mb away on the centromeric side of the distal breakpoint. The centromeric side of the proximal breakpoint contains 11 kb of LINE elements, so there are other very closely related sequences from other regions of chromosome 8 and other chromosomes that match with the relatively short sequence of the PCR product on the centromeric side of the breakpoint. But the sequence directly adjacent to the breakpoint is the only one on chromosome 8 that perfectly matches with the sequence of the PCR product, and the size of the PCR product is exactly what is predicted from the genomic sequence. These results confirm that the proximal breakpoint is 5 kb centromeric of probe b (Figure 1A) and the distal breakpoint is 444 bp from the telomeric end of *Eco*RI fragment 3 (Figure 2A). They also indicate that the 10-Mb region between the proximal and distal breakpoints has been inverted on the *Os* chromosome. There is only

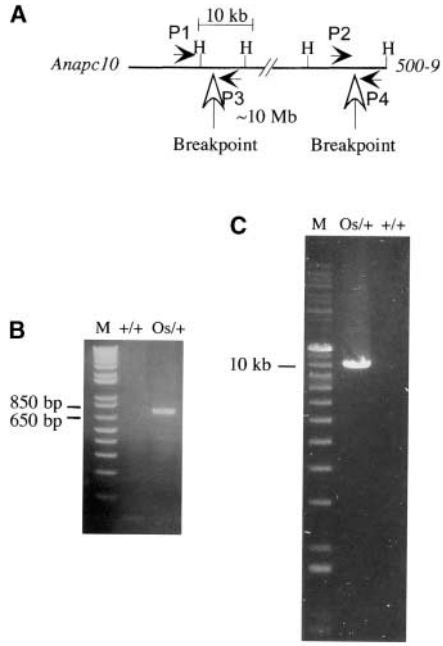

FIGURE 4.—Amplification of *Os*-specific fragments with primers from the proximal and distal breakpoint regions. (A) Diagram of the breaks and the relative position of primers. Centromere to telomere is left to right. (B) PCR of *Os*/+ and +/+ mouse DNA with primers p1 and p2 located on the centromeric side of the proximal and distal breaks. (C) PCR of *Os*/+ and +/+ mouse DNA with primers p3 and p4 located on the telomeric side of the proximal and distal breaks. The location of the primers is shown in their normal orientation. A PCR product will be amplified by these primers only if the ends of the broken fragments are joined through an inversion.

a small loss of sequences at each breakpoint (13 bp at the distal breakpoint and 29 bp at the proximal breakpoint). The normal sequence spanning the proximal breakpoint contains a LINE element. In addition to the 11 kb of LINE elements on the centromeric side of this breakpoint, 5 kb of LINE elements are on the telomeric side. The normal sequence spanning the distal breakpoint also contains a LINE element and a number of LINE elements are interspersed in the nearby sequence on either side. There is no homology, however, between the sequences directly at the proximal and distal breakpoints.

Genes between *Anapc10* and 500-9 show no evidence of loss and rearrangement in *Os* mice: A schematic of the rearrangement, based on the sequence information and our molecular analysis of *Os* mice, is shown in Figure 6. We used genes within the *Anapc10*–500-9 segment as additional molecular probes to determine if this segment is intact in *Os* mice. The Hedgehog-interacting protein (*Hhip*) gene (CHUANG and MCMAHON 1999) is the closest confirmed gene 3′ of *Anapc10* and is located ~200 kb away on the telomeric side of the *Anapc10* locus. The mouse *Spalt-like 1* (*Sall1*) gene (BUCK *et al.* 2000) is the closest confirmed gene on the left (centromere-proximal) flank of 500-9 and is located >400 kb away from the 500-9 breakpoint (Figure 6). Southern analysis of *Os*/+ DNA with cDNA clones of mouse *Hhip* (EST BU053222) and *Sall1* (EST AI426947) genes demonstrated that both genes have normal structure and copy number in *Os*/+ mice (not shown), further strengthening our conclusion that the rearrangement in *Os* mice is not accompanied by loss of sequences between the breakpoints. We also detected no rearrangement or loss of the *Abce1* gene (using EST AI930292 as a probe), located close (centromere proximal) to the proximal *Os* breakpoint, but outside of the inverted segment (Figure 6). This is in agreement with an earlier report demonstrating retention (and lack of recombination) of strain 101-specific polymorphisms over a large segment of DNA, including the *Anapc10*–500-9 region (LENZ *et al.* 1998).

Cytogenetic analysis of the *Os* mutation: The G-banding pattern of chromosome 8 in *Os* mice has been described as grossly normal (LENZ *et al.* 1998). The exact positions of the *Anapc10* and 500-9 loci on the cytogenetic map of chromosome 8 are currently unknown. According to Map Viewer (http://ncbi.nlm.nih.gov) the positions of the proximal and distal *Os* breakpoint regions (*Anapc10* and 500-9) would be in bands C1 and C3, respectively, whereas according to Ensembl (http://www.ensembl.org) these loci would reside in bands C3 and C5. An ideogram of chromosome 8 is shown in Figure 7A. Our analysis of G-banded chromosomes from liver cultures of *Os* mice indicated some subtle differences in the morphology of the two chromosome 8 homologs, mainly a weaker band C2 in one of the homologs. This difference, however, did not exceed the variability that can be due to technical factors and could not be associated with the normal *vs.* mutant chromosome 8 because of the absence of cytologically distinguishing characteristics of the two chromosomes 8. To distinguish the normal chromosome 8 from its *Os* homolog, we crossed an *Os* female with a male homozygous for a Robertsonian translocation between chromosomes 8 and 12. E15 embryos were classified as normal or *Os* on the basis of their limb phenotype and were used to establish individual cell cultures. The derivation of the cells used for karyotype analysis from an *Os* embryo was confirmed by genotyping (not shown). Examination of G-banded chromosomes of these cells confirmed the weaker appearance of band C2 in one of the homologs and indicated that in the vast majority of the cases, this weakened band is seen on the (free) *Os* chromosome 8 (Figure 7C). Under our conditions of banding, band C4 is not detected (Figure 7B). A very faint band distal to C2, however, was observed in some of the cells on the *Os* chromosome 8 (*e.g.*, the *Os* chromosome in Figure 7D). These observations, together with our molecular analysis described above, lead us to propose the following explanation of the cytogenetic observations: one of the breaks of the *Os* inversion is located in band 8C2, whereas the other break is in an adjacent G-light band. The inversion would split band C2, accounting

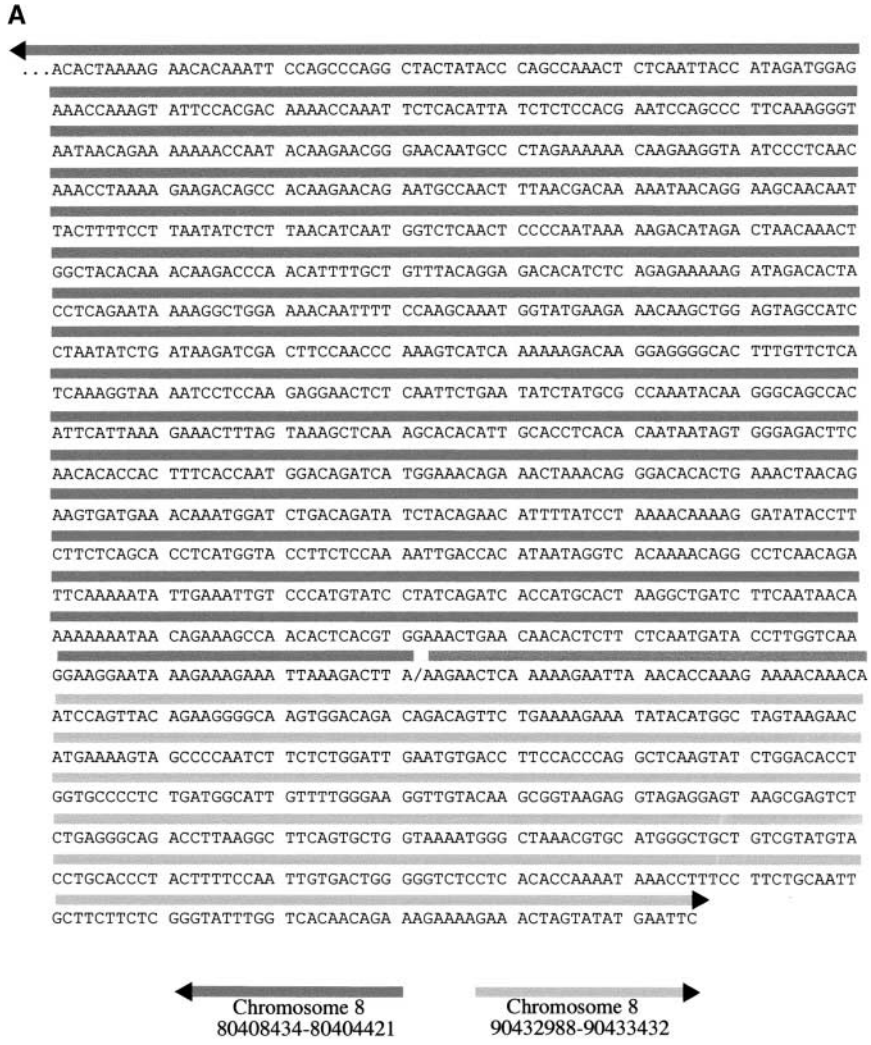

FIGURE 5.—Sequence across the proximal and distal breakpoints. (A) Sequence from the distal breakpoint PCR product. (B) Sequence from the proximal breakpoint PCR product. Arrows in dark gray indicate sequence from the inverted segment of chromosome 8. Arrows in light gray are from noninverted sequence. The direction of the arrows indicates the direction of the sequence on normal chromosome 8, from centromere to telomere. Numbers indicate the corresponding sequence on chromosome 8. The slash in each sequence indicates where the breakpoint is. Only part of the distal breakpoint PCR product sequence is shown.

for its weak appearance. The origin of the very faint band distal to C2 is less certain. It could represent the distal portion of band 8C2 in its inverted position, perhaps juxtaposed to the difficult-to-detect band C4. According to this interpretation, the second break would occur in the light band, which in our preparations corre-

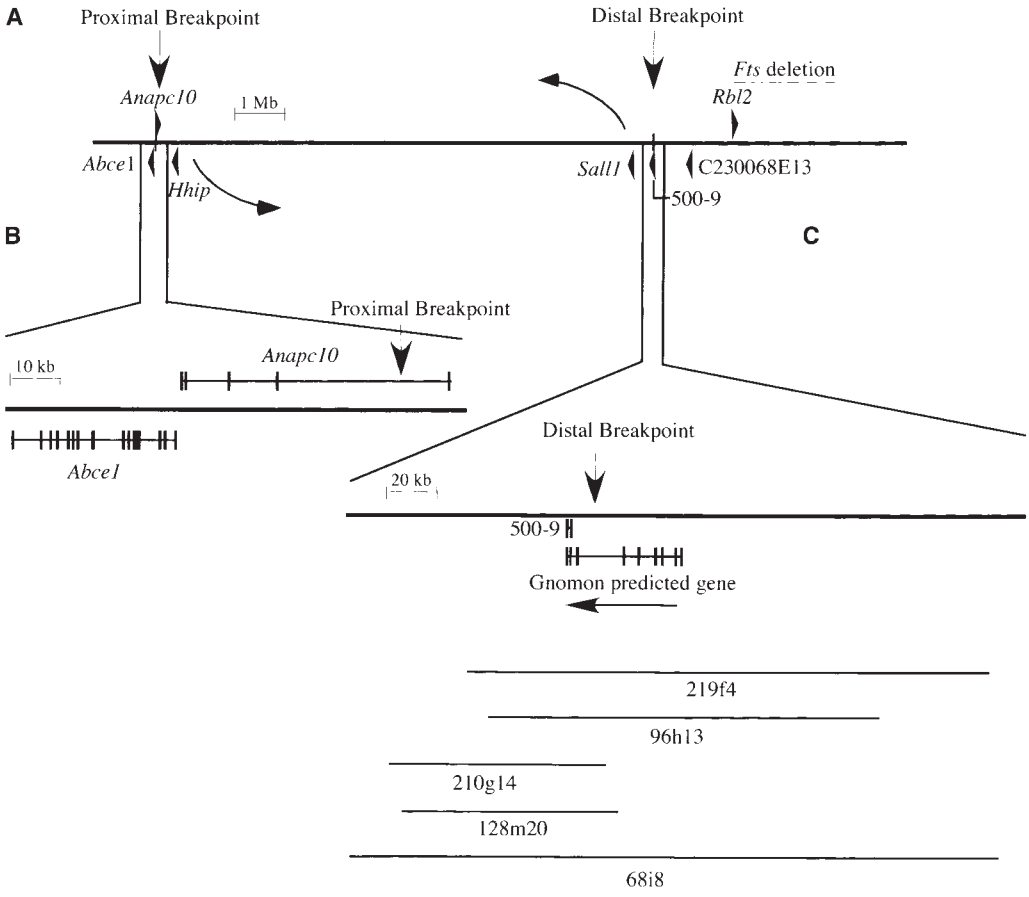

FIGURE 6.—Map of the *Anapc10*–500-9 region. (A) Position of *Anapc10*, 500-9, and neighboring genes (see text) on the physical map of chromosome 8. Only genes in the vicinity of the breakpoints (indicated by arrows) are shown. *Anapc10* and 500-9 are separated by ~9.9 Mb (http://ncbi.nlm.nih.gov). The *Fts* deletion (PETERS *et al.* 2002) is indicated by a dashed line. (B) Detailed view of the proximal breakpoint region. *Anapc10* and *Abce1* are separated by <200 bp and are transcribed from opposite strands. The proximal *Os* breakpoint is located within a large intron of *Anapc10* (PRAVTCHEVA and WISE 2001). Some of the exons of *Abce1* are very closely spaced and cannot be resolved on this scale. (C) Detailed view of the distal breakpoint region. The position of the Gnomon-predicted gene hnm39311 that includes the 500-9 novel sequence is indicated. The distal breakpoint is located within an intron of this hypothetical gene. 219f4, 96h13, 210g14, 128m20, and 68i8 are BAC clones from the 500-9 region. The extent of the BAC clones was determined by sequencing of the BAC ends and comparing the sequence with the assembled mouse genome sequence.

sponds to the region C3-C5. The faint distal band may also be due to an effect of the rearrangement on the degree of contraction of this segment of the chromosome, which might make the usually elusive band 8C4 somewhat easier to detect.

The different phenotypes of 94-A/K and *Os* mice are not due to strain background effects on the mutation: The identification of a second chromosome region affected by the rearrangement present in *Os* suggested that the more complex phenotype of these mice may be due to the involvement of additional genes. It remained possible, however, that the different phenotypes of 94-A/K and *Os* are the result of strain background effects on the haplo-insufficiency of *Anapc10*. To determine the effect of the FVB/N strain background on the *Os* phenotype, we have backcrossed *Os* mice from the ROP/Le-Os Es 1^a/+ Es 1^a/J with FVB/N mice for seven generations, with the goal of producing a congenic FVB/N *Os* strain. There has been no disappearance or amelioration of the dominant effects of *Os*, except for a greater tendency for splitting at the distal end of the fused digits 2 and 3 on the front legs (which remain unambiguously syndactylous). In addition, we noticed a decline in the number of surviving *Os* mice in the colony after 3 months. A more controlled comparison of the life span of *Os* mice on their original background and on the FVB/N background is in progress. We have not observed a similar effect of the 94-A/K mutations on the life span of the mice. These results clearly indicate that the absence of dominant effects in 94-A/K mice is not due to the ameliorating influence of their FVB/N genetic background on *Anapc10* haplo-insufficiency and indicate that, if anything, the FVB/N background may aggravate the dominant effects of *Os*. Inactivation of the

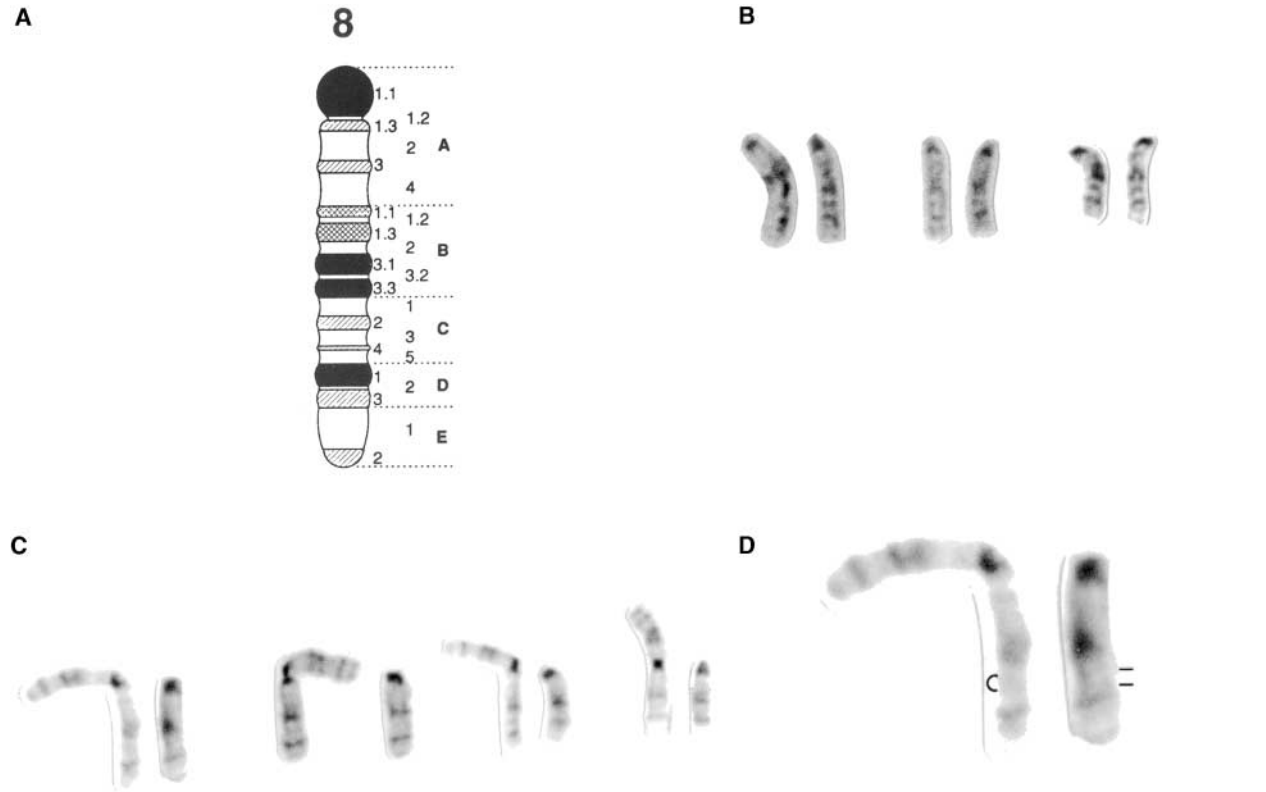

FIGURE 7.—Cytogenetic analysis of the *Os* mutation. (A) Ideogram of chromosome 8 (from LYON *et al.* 1996). (B) G-banded chromosomes 8 from wt cells. (C) Chromosome 8 pairs from e15 *Os* embryos from a cross between an Rb(8.12) homozygous male and an *Os*/+ female. The Rb(8.12) chromosome is shown on the left. In all pairs shown in C, band 8C2 appears weaker on the *Os* chromosome. (D) Magnified view of the first chromosome pair shown in C. A faint distal band (at the approximate position of the usually undetectable band C4) can be seen on the *Os* chromosome 8. A semicircle marks band 8C2 on the normal chromosome 8; short lines mark the position of the two weak bands that can be seen on the mutant chromosome 8.

gene encoding another component of the APC/C, APC2, is also not associated with abnormalities in the heterozygous state (WIRTH *et al.* 2004).

Transcribed sequences from the region surrounding the distal breakpoint on chromosome 8: Comparison of the sequence of the 500-9 RACE clone with the mouse genomic sequence indicates that the novel portion of the cDNA sequence spans a small intron. The presence of this intron is confirmed by the small difference in size observed between DNA and RT-PCR products (Figure 8). The computer program Genscan also predicts the position of the intron and identifies the 3′ exon as a terminal exon. These data thus suggest that either the 500-9 sequence is derived from a gene that has been disrupted by the *Os* rearrangement or cryptic splice sites have been activated by the rearrangement. Hybridization of the 500-9 novel sequence to multiple tissue Northerns and embryo Northerns of normal mice did not detect an unambiguous signal (a broad smear was detected at low stringency), whereas hybridization to tissue Northerns from *Os*/+ mice detected the abnormal, short mRNA species with the *Anapc10* 5′ end (not shown). We have so far been able to detect only very weak expression of the 500-9 transcript in some normal tissues by RT-PCR and we have not been able to detect any longer versions of this transcript by 5′ or 3′ RACE in normal mice.

We used two additional approaches to identify transcribed sequences from the distal chromosome 8 region: (i) screening of a day e10–e12 cDNA library made in the laboratory with the 500-9 sequence [four identical

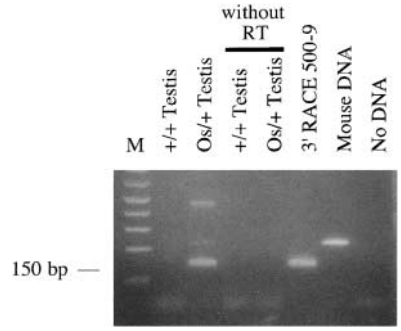

FIGURE 8.—Expression analysis of 500-9. RT-PCR of testis RNA from normal and *Os*/+ mice with 500-9 sequence primers is shown. An RT-PCR product is visible only in the *Os*/+ lane. The RT-PCR product is smaller than the amplified genomic DNA fragment, as a result of splicing.

clones of ~1 kb (two of them designated R1 and R5), which include the 500-9 sequence, were isolated] and (ii) cDNA selection with one of the distal chromosome 8 BACs (96h13; Figure 6). Three of the 30 cDNA clones with homology to the BAC (15, 64/3, and 84) were located in proximity to the distal break (Figure 2). All of the isolated cDNAs (including R1/R5), however, are not spliced and lack large open reading frames. We have not detected a clear signal on multiple tissue Northerns or embryo Northerns from normal mice with any of these clones. They also show no homology to cDNA sequences or ESTs in the public database. The 16-kb *Hin*dIII fragment containing the distal *Os* breakpoint contains a sequence of 313 bp that is 87% identical to a segment in the orthologous region of human chromosome 16. Several characteristics of the cDNA clones from this region—lack of correspondence to annotated genes, lack of ESTs in the public database, low-level and difficult-to-detect transcription, absence of long ORFs, and proximity to evolutionarily conserved noncoding sequences—are similar to the characteristics of a recently described class of transcripts in humans (Kapranov *et al.* 2002; Kampa *et al.* 2004). Although there are a large number of such transcripts, their function is currently unknown.

Known and predicted genes in the vicinity of the distal *Os* breakpoint: There are no known genes in the distal breakpoint region, but there are several predicted genes in the vicinity of the breakpoint. One of the predicted genes (hmn39311) that would be the strongest candidate for the dominant effects of *Os* is shown in Figure 6C. The gene is predicted to contain 9 exons, and sequences from the last two exons are present in the 500-9 transcript (where they are spliced in a manner identical to that of the predicted transcript). This hypothetical gene would be interrupted by the *Os* rearrangement in an intron (Figure 6) and its 3′ portion would be placed in the correct transcriptional orientation with regard to *Anapc10* as a result of the inversion. The predicted protein shows some homology to a hepatocyte growth factor-related gene, Livertine (Ruiz i Altaba and Thery 1996). No ESTs with homology to the predicted mRNA are present in the public databases, and there is no analogous gene prediction in the corresponding region of human chromosome 16. We have so far detected no transcripts from this predicted gene by RT-PCR. Several additional predicted genes are in proximity to the breakpoint (not shown). The closest ESTs are located ~41 kb centromeric and ~75 kb telomeric to this predicted gene and are unspliced (UCSC web site: http://genome.ucsc.edu). There are also no CpG islands in a >500-kb region around the 500-9 sequence (http://genome.ucsc.edu). CpG islands are associated with the promoters of 100% of housekeeping genes and with promoters or internal gene regions of ~40% of the tissue-specific genes (Larsen *et al.* 1992). These data, together with the difficulty we have had so far in identifying transcripts with the 500-9 clone and selected cDNAs from this region, suggest that if transcripts from this region are produced, they are of low abundance and/or restricted expression.

A BAC clone that spans the distal breakpoint does not restore normal development to *Os* mice: One possible explanation for the dominant effects of *Os* is that they are due to haplo-insufficiency of a gene(s) at the distal break inactivated as a result of the rearrangement. If so, it should be possible to restore normal development in *Os* mice by providing an additional copy of the inactivated gene. To determine if this will be the case, we micro-injected FVB/N mouse embryos with a linearized mouse BAC clone (96h13) that spans the distal break in the *Os* chromosome 8. We identified four founders by PCR with primers from the vector sequences (not shown). None of the transgenic founders or their progeny exhibited any obvious abnormalities. The extent of the injected sequences retained in the individual founders was determined by Southern hybridization with probes from both ends of the linearized construct and with a probe within the 16-kb *Hin*dIII fragment (cDNA clone 64-3; not shown). Two of the lines, 4 and 6, gave a positive signal with all of the probes, indicating that they probably have retained intact BAC copies. A cross between a line 4 male and an *Os* female produced a litter of nine, five of which were phenotypically *Os*. Two of the *Os* mice had also inherited the 96h13 transgene. There was no apparent difference in the phenotype of these two mice compared with their transgene-negative *Os* littermates. We have also crossed homozygous females from transgenic line 6 with an *Os* male at the N5 generation of backcrossing with FVB/N. Six of 11 mice from this cross were phenotypically *Os*, despite the fact that all of them contained one copy of the transgene. In addition, four of the six *Os* mice were dead by the age of 7 weeks (while none of the wt mice had died by that time), indicating that they have a shortened life similar to the *Os* mice backcrossed to FVB/N (see above). This analysis indicated that the presence of the transgene does not restore normal development to mice with the *Os* mutation.

DISCUSSION

The radiation-induced *Os* mutation has a complex phenotype, affecting cell cycle progression and limb and kidney development. The results presented here further characterize the rearrangement in *Os* mice, as a step toward identifying the mechanism by which it disrupts normal development.

We have determined that the novel 500-9 sequence from the *Os*-specific hybrid transcript originates from a genomic region that is normally ~5 cM (by genetic mapping) and ~10 Mb (by physical mapping) telomeric to the *Anapc10* locus on chromosome 8 (Figure 6). Molecular analysis of *Os*/+ DNA with probes flanking

the proximal and distal breaks and within the intervening 10-Mb segment showed no evidence for loss of sequences as a result of the *Os* rearrangement (Figures 1 and 2). We have presented molecular evidence that the *Os* mutation is associated with a chromosome inversion (Figures 4 and 5). One break of this inversion is within an intron of the *Anapc10* gene, whereas the other break is a few kilobases telomeric to the 500-9 sequence (Figures 1, 2, and 4–6). These results are in agreement with previous studies (Lenz *et al.* 1998) that have shown suppression of recombination between the normal and mutant chromosomes 8 over a region of 12–27 cM, leading these authors to hypothesize an inversion. The region showing suppression of recombination in this previous report (defined on the centromeric side by the recombining marker D8Mit193 and on the telomeric side by the nonrecombining D8Mit210) spans the *Anapc10* and 500-9 loci and extends further in both the centromeric (~6 Mb) and the telomeric (5–6 Mb) direction. The size of the nonrecombinant flanks of the inversion is comparable to the estimated size of the genomic segment of donor origin retained in a congenic strain (Flaherty 1981).

Comparison of the 500-9 transcript sequence with that of genomic DNA indicates that 500-9 contains two exons separated by a small intron. The 500-9 sequence and four unspliced cDNAs isolated by cDNA library screening show overlap with a Gnomon-predicted transcript in the 500-9 region (Figure 6). The inversion would place the 3′ portion of the predicted gene, including the 500-9 sequence, in proximity to and in the same transcriptional orientation as the *Anapc10* gene (Figure 6). While these results support the idea that the 500-9 sequence is part of a normal gene that has been interrupted as a result of the *Os* rearrangement, so far we have not been able to unambiguously identify a transcript corresponding to the 500-9 sequence in any tissues of normal mice by Northern analysis or RACE. A large number of low-level transcripts that map outside of annotated exonic and EST sequences was found in a study of the transcriptional activity of human chromosomes 21 and 22 (Kapranov *et al.* 2002; Kampa *et al.* 2004), and they share some of the characteristics of the 500-9 region cDNA clones. Further analysis of these cDNAs will determine what is the effect of the *Os* rearrangement on their transcription and what if any role they play in the *Os* phenotype.

If a gene in this region is interrupted and inactivated by the rearrangement, the abnormal *Os* phenotype would be due to haplo-insufficiency for this gene's product. To test this hypothesis, we have produced transgenic mice with one of the 500-9 region BACs (96h13; Figure 6). The transgenes, however, were not able to restore normal development to *Os* mice. While a positive effect of the transgene would have been informative, the lack of an effect is less so. It could indicate that the transgene did not contain the interrupted gene and its regulatory elements in their entirety or that the abnormal *Os* phenotype is caused by another mechanism, *e.g.*, abnormal activation of a neighboring gene or the production of a hybrid protein with novel properties. The latter possibility can be addressed by producing transgenic mice that express the abnormal hybrid transcript.

Genes located near the rearrangement breakpoints may be affected through long-range effects on their expression. The nearest confirmed gene 3′ of *Anapc10* is the *Hhip* gene, at a distance of ~200 kb (Figure 6). *Hhip* encodes the hedgehog- interacting protein, which is an important modulator of the signaling from all three vertebrate hedgehog genes [*Sonic hedgehog* (*Shh*), *Indian hedgehog* (*Ihh*), and *Desert hedgehog* (*Dhh*)] and attenuates their effects (Chuang and McMahon 1999; Chuang *et al.* 2003). *Shh* plays an important role in limb morphogenesis (Capdevila and Izpisua Belmonte 2001; Ingham and McMahon 2001; Sanz-Ezquerro and Tickle 2001; Litingtung *et al.* 2002). Interestingly, several mouse mutations affecting limb patterning have been associated with long-range position effect on the activity of *Ihh* or *Shh* over a distance of 1.3–1.8 cM (Yang *et al.* 1998; Sharpe *et al.* 1999; Lettice *et al.* 2002, 2003).

The *Abce1* gene (ATP-binding cassette, subfamily E, member 1, or ribonuclease L inhibitor, *RNS4I, Rli*) is located in close proximity to the 5′ end of *Anapc10* and is transcribed in the opposite orientation (Figure 6). *Abce1* belongs to a family of proteins that contain a conserved ATP-binding domain, and many are believed to function as transporters across cell membranes (Schriml and Dean 2000). *Abce1* is an inhibitor of ribonuclease L (Bisbal *et al.* 1995), and both play a role in controlling cell differentiation (Bisbal *et al.* 2000). We have not detected any difference in *Abce1* expression between normal and *Os* adult tissues (our unpublished observations).

Sall1 is located ~400 kb away from 500-9 (Figure 6) and is the closest confirmed gene on its centromeric side. The human homolog of *Sall1* (*SALL1*) has been implicated in a developmental syndrome with limb and kidney involvement [Townes-Brocks syndrome (TBS); Kohlhase *et al.* 1998]. Mice that lack the *mSall1* gene (Nishinakamura *et al.* 2001) failed to develop kidneys, but showed no abnormalities in their limbs. On the other hand, a targeted mutation producing a truncated *Sall1* protein similar to the one found in TBS patients resulted in abnormal kidney and limb development (Kiefer *et al.* 2003). A position effect on *SALLI* extending over ~180 kb has been described in a patient with Townes-Brocks syndrome (Marlin *et al.* 1999). The closest gene known to code for a protein on the telomeric side of 500-9 (C230068E13) is located ~770 kb away.

The results presented here also clarify the relative chromosome position of *Os* and another mutation on chromosome 8 associated with abnormal limb development, *Fused toes* (*Fts*; Van der Hoeven *et al.* 1994). *Fts*

mice have a complex phenotype, including digit fusions and thymic hyperplasia in heterozygotes and brain malformations accompanied by death at midgestation in homozygotes. This transgene-induced mutation is associated with a 1.6-Mb deletion (Lesche *et al.* 1997; Peters *et al.* 2002). The *Rbl2* gene, adjacent to the proximal end of the *Fts*-associated deletion, is located >1.6 Mb distal to 500-9 in the mouse chromosome 8 sequence (http://ncbi.nlm.nih.gov; Figure 6). Thus the chromosome segments affected by the *Os*-associated inversion and the *Fts*-associated deletion are nonoverlapping. Earlier genetic analysis with probes from the *Fts* breakpoint and deleted segment had indicated that both are unaltered in *Os* mice (Lesche and Rüther 1998).

In summary, molecular analysis of the radiation-induced *Os* mutation indicates that it is associated with two breaks on chromosome 8 that are ~5 cM (~10 Mb) apart. No loss of sequences in the intervening fragment has been detected in *Os* mice. Southern analysis, PCR, junction fragment sequencing, and the production of a hybrid transcript containing sequences that were originally 10 Mb apart and in the opposite orientation indicate that the radiation-induced *Os* mutation is associated with a chromosome inversion. Genes interrupted by the breaks or in proximity to the breakpoints (*Hhip*, *Abce1*, and *Sall1*) need to be examined for their involvement in the dominant effects of this mutation.

We thank Daniel Kerr and Xiaoping Shen for excellent technical assistance and Hui Feng Li for her care of the mice. This work was supported by a grant from the March of Dimes Birth Defects Foundation to D.P. and in part by funds from the New York State Office of Mental Retardation and Developmental Disabilities.

LITERATURE CITED

Barsky, A. J., 1958 *Congenital Abnormalities of the Hand and Their Surgical Treatment.* Charles C. Thomas, Springfield, IL.

Bernstein, J., 1992 Renal hypoplasia and dysplasia, pp. 1121–1137 in *Pediatric Kidney Disease*, edited by C. M. Edelmann, Jr. Little Brown & Co., Boston.

Bisbal, C., C. Martinand, M. Silhol, B. Lebleu and T. Salehzada, 1995 Cloning and characterization of a RNAse L inhibitor. A new component of the interferon-regulated 2–5A pathway. J. Biol. Chem. **270:** 13308–13317.

Bisbal, C., M. Silhol, H. Laubenthal, T. Kaluza, G. Carnac *et al.*, 2000 The 2′-5′ oligoadenylate/RNase L/RNase L inhibitor pathway regulates both MyoD mRNA stability and muscle cell differentiation. Mol. Cell. Biol. **20:** 4959–4969.

Buck, A., L. Archangelo, C. Dixkens and J. Kohlhase, 2000 Molecular cloning, chromosomal localization, and expression of the murine SALL1 ortholog Sall1. Cytogenet. Cell Genet. **89:** 150–153.

Capdevila, J., and J. C. Izpisua Belmonte, 2001 Patterning mechanisms controlling vertebrate limb development. Annu. Rev. Cell Dev. Biol. **17:** 87–132.

Ceci, J. D., and K. A. Mills, 1997 Mouse chromosome 8. Mamm. Genome **7:** 5143–5158.

Cheng, S., Y. Chen, J. A. Monforte, R. Higuchi and B. Van Houten, 1995 Template integrity is essential for PCR amplification of 20- to 30-kb sequences from genomic DNA. PCR Methods Appl. **4:** 294–298.

Chomczynski, P., and N. Sacchi, 1987 Single-step method of RNA isolation by acid guanidinium thiocyanate-phenol-chloroform extraction. Anal. Biochem. **162:** 156–159.

Chuang, P. T., and A. P. McMahon, 1999 Vertebrate Hedgehog signalling modulated by induction of a Hedgehog-binding protein. Nature **397:** 617–621.

Chuang, P. T., T. Kawcak and A. P. McMahon, 2003 Feedback control of mammalian Hedgehog signaling by the Hedgehog-binding protein, Hip1, modulates Fgf signaling during branching morphogenesis of the lung. Genes Dev. **17:** 342–347.

Davis, L. G., M. D. Dibner and J. F. Battey, 1986 *Basic Methods in Molecular Biology.* Elsevier Science, New York.

Falconer, D. S., M. Latyszewski and J. H. Isaacson, 1964 Diabetes insipidus associated with Oligosyndactylism in the mouse. Genet. Res. **5:** 473–488.

Feinberg, A. P., and B. Vogelstein, 1983 A technique for radiolabeling DNA restriction endonuclease fragments to high specific activity. Anal. Biochem. **132:** 6–13.

Flaherty, L., 1981 Congenic strains, pp. 215–222 in *The Mouse in Biomedical Research*, Vol. 1, edited by H. L. Foster, J. D. Small and J. G. Fox. Academic Press, New York.

Frohman, M. A., 1990 RACE: rapid amplification of cDNA ends, pp. 28–38 in *PCR Protocols: A Guide to Methods and Applications*, edited by M. A. Innis, D. H. Gelfand, J. J. Sninsky and T. J. White. Academic Press, New York.

Grossberger, R., C. Gieffers, W. Zachariae, A. V. Podtelejnikov, A. Schleiffer *et al.*, 1999 Characterization of the DOC1/APC10 subunit of the yeast and the human anaphase-promoting complex. J. Biol. Chem. **274:** 14500–14507.

Grüneberg, H., 1956 Genetical studies on the skeleton of the mouse. XVIII. Three genes for syndactylism. J. Genet. **54:** 113–145.

Grüneberg, H., 1961 Genetical studies on the skeleton of the mouse. XXVII. The development of Oligosyndactylism. Genet. Res. **2:** 33–42.

Gurrieri, F., K. W. Kjaer, E. Sangiorgi and G. Neri, 2002 Limb anomalies: Developmental and evolutionary aspects. Am. J. Med. Genet. **115:** 231–244.

Hiraoka, L., W. Golden and T. Magnuson, 1989 Spindle pole organization during early mouse development. Dev. Biol. **133:** 24–36.

Hogan, B., R. Beddington, F. Costantini and E. Lacy, 1994 *Manipulating the Mouse Embryo: A Laboratory Manual*, Ed. 2. Cold Spring Harbor Laboratory Press, Cold Spring Harbor, NY.

Hwang, L. H., and A. W. Murray, 1997 A novel yeast screen for mitotic arrest mutants identifies DOC1, a new gene involved in cyclin proteolysis. Mol. Biol. Cell **8:** 1877–1887.

Ingham, P. W., and A. P. McMahon, 2001 Hedgehog signaling in animal development: paradigms and principles. Genes Dev. **15:** 3059–3087.

Irniger, S., S. Piatti, C. Michaelis and K. Nasmyth, 1995 Genes involved in sister chromatid separation are needed for B-type cyclin proteolysis in budding yeast. Cell **81:** 269–278.

Kadam, K. M., 1962 Genetical studies on the skeleton of the mouse. XXXI. The muscular anatomy of syndactylism and Oligosyndactylism. Genet. Res. **3:** 139–156.

Kampa, D., J. Cheng, P. Kapranov, M. Yamanaka, S. Brubaker *et al.*, 2004 Novel RNAs identified from an in-depth analysis of the transcriptome of human chromosomes 21 and 22. Genome Res. **14:** 331–342.

Kapranov, P., S. E. Cawley, J. Drenkow, S. Bekiranov, R. L. Strausberg *et al.*, 2002 Large-scale transcriptional activity in chromosomes 21 and 22. Science **296:** 916–919.

Kiefer, S. M., K. K. Ohlemiller, J. Yang, B. W. McDill, J. Kohlhase *et al.*, 2003 Expression of a truncated SallI transcriptional repressor is responsible for Townes-Brocks syndrome birth defects. Hum. Mol. Genet. **12:** 2221–2227.

King, R. W., J.-M. Peters, S. Tugendreich, M. Rolfe, P. Hieter *et al.*, 1995 A 20S complex containing CDC27 and CDC16 catalyzes the mitosis-specific conjugation of ubiquitin to cyclin B. Cell **81:** 279–288.

King, R. W., R. J. Deshaies, J. M. Peters and M. W. Kirschner, 1996 How proteolysis drives the cell cycle. Science **274:** 1652–1659.

Kohlhase, J., A. Wischermann, H. Reichenbach, U. Froster and W. Engel, 1998 Mutations in the SALL1 putative transcription factor gene cause Townes-Brocks syndrome. Nat. Genet. **18:** 81–83.

Kominami, K., H. Seth-Smith and T. Toda, 1998 Apc10 and Ste9/Srw1, two regulators of the APC-cyclosome, as well as the CDK

inhibitor Rum1 are required for G1 cell-cycle arrest in fission yeast. EMBO J. **17:** 5388–5399.

Konishi, Y., J. Stegmuller, T. Matsuda, S. Bonni and A. Bonni, 2004 Cdh1-APC controls axonal growth and patterning in the mammalian brain. Science **303:** 1026–1030.

Larsen, F., G. Gundersen, R. Lopez and H. Prydz, 1992 CpG islands as gene markers in the human genome. Genomics **13:** 1095–1107.

Lenz, O., U. Teichmann, A. Langers, L. J. Striker and W. J. Pavan, 1998 Linkage disequilibrium mapping reveals suppressed recombination at the Os locus. Mamm. Genome **9:** 681–682.

Lesche, R., and U. Rüther, 1998 The dominant mouse mutations Fused toes (Ft) and oligosyndactylism (Os) are not allelic. Mamm. Genome **9:** 588–589.

Lesche, R., A. Peetz, F. van der Hoeven and U. Ruther, 1997 Ft1, a novel gene related to ubiquitin-conjugating enzymes, is deleted in the Fused toes mouse mutation. Mamm. Genome **8:** 879–883.

Lettice, L. A., T. Horikoshi, S. J. Heaney, M. J. van Baren, H. C. van der Linde *et al.*, 2002 Disruption of a long-range cis-acting regulator for Shh causes preaxial polydactyly. Proc. Natl. Acad. Sci. USA **99:** 7548–7553.

Lettice, L. A., S. J. Heaney, L. A. Purdie, L. Li, P. de Beer *et al.*, 2003 A long-range Shh enhancer regulates expression in the developing limb and fin and is associated with preaxial polydactyly. Hum. Mol. Genet. **12:** 1725–1735.

Litingtung, Y., R. D. Dahn, Y. Li, J. F. Fallon and C. Chiang, 2002 Shh and Gli3 are dispensable for limb skeleton formation but regulate digit number and identity. Nature **418:** 979–983.

Lyon, M. F., S. H. Rastan and S. D. M. Brown, 1996 *Genetic Variants and Strains of the Laboratory Mouse*, Ed. 3. Oxford University Press, Oxford.

Magnuson, T., and C. J. Epstein, 1984 Oligosyndactyly: a lethal mutation in the mouse that results in mitotic arrest very early in development. Cell **38:** 823–833.

Manouvrier-Hanu, S., M. Holder-Espinasse and S. Lyonnet, 1999 Genetics of limb anomalies in humans. Trends Genet. **15:** 409–417.

Marlin, S., S. Blanchard, R. Slim, D. Lacombe, F. Denoyelle *et al.*, 1999 Townes-Brocks syndrome: detection of a SALL1 mutation hot spot and evidence for a position effect in one patient. Hum. Mutat. **14:** 377–386.

Maruyama, K., and S. Sugano, 1994 Oligo-capping: a simple method to replace the cap structure of eukaryotic mRNAs with oligoribonucleotides. Gene **138:** 171–174.

Morgan, D. O., 1999 Regulation of the APC and the exit from mitosis. Nat. Cell Biol. **1:** E47–E53.

Nasmyth, K., J. M. Peters and F. Uhlmann, 2000 Splitting the chromosome: cutting the ties that bind sister chromatids. Science **288:** 1379–1385.

Nishinakamura, R., Y. Matsumoto, K. Nakao, K. Nakamura, A. Sato *et al.*, 2001 Murine homolog of SALL1 is essential for ureteric bud invasion in kidney development. Development **128:** 3105–3115.

Passmore, L. A., E. A. McCormack, S. W. N. Au, A. Paul, K. R. Willison *et al.*, 2003 Doc1 mediates the activity of the anaphase-promoting complex by contributing to substrate recognition. EMBO J. **22:** 786–796.

Paterson, H. F., 1979 In vivo and in vitro studies on the early embryonic lethal Oligosyndactylism (Os) in the mouse. J. Embryol. Exp. Morphol. **52:** 115–125.

Peters, T., K. Ausmeier, R. Dildrop and U. Ruther, 2002 The mouse Fused toes (Ft) mutation is the result of a 1.6-Mb deletion including the entire Iroquois B gene cluster. Mamm. Genome **13:** 186–188.

Peterson, A. S., 1998 Direct cDNA selection, pp. 159–190 in *Genome Analysis. A Laboratory Manual, Volume 2: Detecting Genes*, edited by B. Birren, E. D. Green, S. Klapholz, R. M. Myers and J. Roskams. Cold Spring Harbor Laboratory Press, Cold Spring Harbor, NY.

Pravtcheva, D. D., and T. L. Wise, 1995 A postimplantation lethal mutation induced by transgene insertion on mouse chromosome 8. Genomics **30:** 529–544.

Pravtcheva, D. D., and T. L. Wise, 1996 A transgene-induced mitotic arrest mutation in the mouse allelic with *Oligosyndactylism*. Genetics **144:** 1747–1756.

Pravtcheva, D. D., and T. L. Wise, 2001 Disruption of Apc10/Doc1 in three alleles of Oligosyndactylism. Genomics **72:** 78–87.

Ruiz i Altaba, A., and Thery, C., 1996 Involvement of Livertine, a hepatocyte growth factor family member, in neural morphogenesis. Mech. Dev. **60:** 207–220.

Saiki, R. K., 1990 Amplification of Genomic DNA, pp. 13–20 in *PCR Protocols: A Guide to Methods and Applications*, edited by M. A. Innis, D. H. Gelfand, J. J. Sninsky and T. J. White. Academic Press, New York.

Sambrook, J., E. F. Fritsch and T. Maniatis, 1989 *Molecular Cloning: A Laboratory Manual*, Ed. 2. Cold Spring Harbor Laboratory Press, Cold Spring Harbor, NY.

Sanz-Ezquerro, J. J., and C. Tickle, 2001 "Fingering" the vertebrate limb. Differentiation **69:** 91–99.

Schriml, L. M., and M. Dean, 2000 Identification of 18 mouse ABC genes and characterization of the ABC superfamily in Mus musculus. Genomics **64:** 24–31.

Sharpe, J., L. Lettice, J. Hecksher-Sorensen, M. Fox, R. Hill *et al.*, 1999 Identification of sonic hedgehog as a candidate gene responsible for the polydactylous mouse mutant Sasquatch. Curr. Biol. **9:** 97–100.

Sorenson, C. M., S. A. Rogers and M. R. Hammerman, 1996 Abnormal renal development in the Os/+ mouse is intrinsic to the kidney. Am. J. Physiol. **271:** F234–F238.

Stewart, A. D., and J. Stewart, 1969 Studies on syndrome of diabetes insipidus associated with Oligosyndactylism in mice. Am. J. Physiol. **217:** 1191–1198.

Sudakin, V., D. Ganoth, A. Dahan, H. Heller, J. Hershko *et al.*, 1995 The cyclosome, a large complex containing cyclin-selective ubiquitin ligase activity, targets cyclins for destruction at the end of mitosis. Mol. Biol. Cell **6:** 185–197.

Van der Hoeven, F., T. Schimmang, A. Volkmann, M.-G. Mattei, B. Kyewski *et al.*, 1994 Programmed cell death is affected in the novel mouse mutant Fused toes (Ft). Development **120:** 2601–2607.

Van Valen, P., 1966 Oligosyndactylism, an early embryonic lethal in the mouse. J. Embryol. Exp. Morphol. **15:** 119–124.

Wirth, K. G., R. Ricci, J. F. Gimenez-Abian, S. Taghybeeglu, N. R. Kudo *et al.*, 2004 Loss of the anaphase-promoting complex in quiescent cells causes unscheduled hepatocyte proliferation. Genes Dev. **18:** 88–98.

Wise, T. L., and D. D. Pravtcheva, 1997 Perinatal lethality in H19 enhancers-Igf2 transgenic mice. Mol. Reprod. Dev. **48:** 194–207.

Yang, Y., P. Guillot, Y. Boyd, M. F. Lyon and A. P. McMahon, 1998 Evidence that preaxial polydactyly in the Doublefoot mutant is due to ectopic Indian Hedgehog signaling. Development **125:** 3123–3132.

Yee, D., W. Golden, S. Debrot and T. Magnuson, 1987 Short term rescue by RNA injection of a mitotic arrest mutation that affects the preimplantation mouse embryo. Dev. Biol. **122:** 256–261.

Zalups, R. K., 1993 The Os/+ mouse: a genetic animal model of reduced renal mass. Am. J. Physiol. **264:** F53–F60.

Communicating editor: N. A. Jenkins